Neuroradiology (1999) 41: 723–728

K. Okamoto
J. Ito
T. Furusawa
K. Sakai
S. Tokiguchi

Imaging of calvarial eosinophil granuloma

Received: 24 November 1998
Accepted: 5 February 1999

K. Okamoto (✉) · T. Furusawa · K. Sakai
Department of Radiology,
Niigata University School of Medicine,
1-757 Asahimachi-dori, Niigata,
951-8510 Japan
e-mail: nradioko@med.niigata-u.ac.jp
Tel.: + 81-25-227 2315
Fax: + 81-25-227 0788

J. Ito · S. Tokiguchi
Department of Radiology,
Niigata University School of Dentistry,
Niigata, Japan

Abstract We reviewed the imaging of four pathologically proven calvarial eosinophil granulomas. The diameter of the lesions ranged from 13 to 40 mm; three were biconvex, but the other had a collar-stud appearance. Two lesions were in the frontal and two in the parietal bone. On bone-window CT, a bevelled edge was seen in three cases and button sequestration in one, but no sclerotic rim was shown. Although one lesion had a low-density area, the lesions were slightly denser than grey matter. They were isointense with grey or white matter on T1-weighted MRI and gave heterogeneous high signal on proton-density and T2-weighted images. All enhanced markedly, with a less strongly enhancing portion within them. A tail of dural enhancement and reactive change in the overlying galea or temporal muscle were seen in all cases.

Key words Skull · Eosinophilic granuloma · Histiocytosis Langerhans-cell · Computed tomography · Magnetic resonance imaging · Scintigraphy

Introduction

Eosinophil granuloma, Hand-Schüller-Christian disease and Letterer-Siwe disease are characterised by idiopathic proliferation of histiocytes producing focal or systemic manifestations. Collectively, they are called Langerhans-cell histiocytosis (LCH) [1]. The localised form of LCH is commonly referred to as eosinophil granuloma; the term is reserved for cases in which the disease is limited to bone or lung. Accounting for approximately 70 % of cases of LCH, this localised form is the least aggressive expression of the diseases with the best prognosis [1]. Eosinophil granuloma of the skull is most frequently seen in children or adolescents, and its imaging appearances have been described [1–5]. Articles on the MRI appearances of calvarial eosinophil granuloma are sparse [6–11]. We assess the imaging characteristics of eosinophil granuloma of the skull, reviewing four pathologically proven cases.

Materials and methods

We studied three boys and one girl ranging in age from 2 to 10 years (mean 6.7 years), using various imaging techniques. Each patient had a 1 month history of a cranial lump with pain or tenderness. Skull films were obtained in all patients as the initial imaging study. Subsequently CT and MRI were performed. Bone scintigrams with ^{99m}Tc-methylene diphosphonate (MDP), and gallium scintigrams were available for three patients. The diagnosis was confirmed by open biopsy or excision.

MRI was obtained with a 1.5-T system. A dynamic study was performed on two patients, and heavily diffusion-weighted echo-planar images (b = 1200 or 1100 s/mm^2) with a caudocephalad diffusion gradient were also obtained in two cases.

Results

The clinical and radiological features are summarised in Tables 1 and 2. The lesion was solitary and monostotic in all patients: the frontal bone was involved in two, and the parietal bone in the other two. The lesions ranged

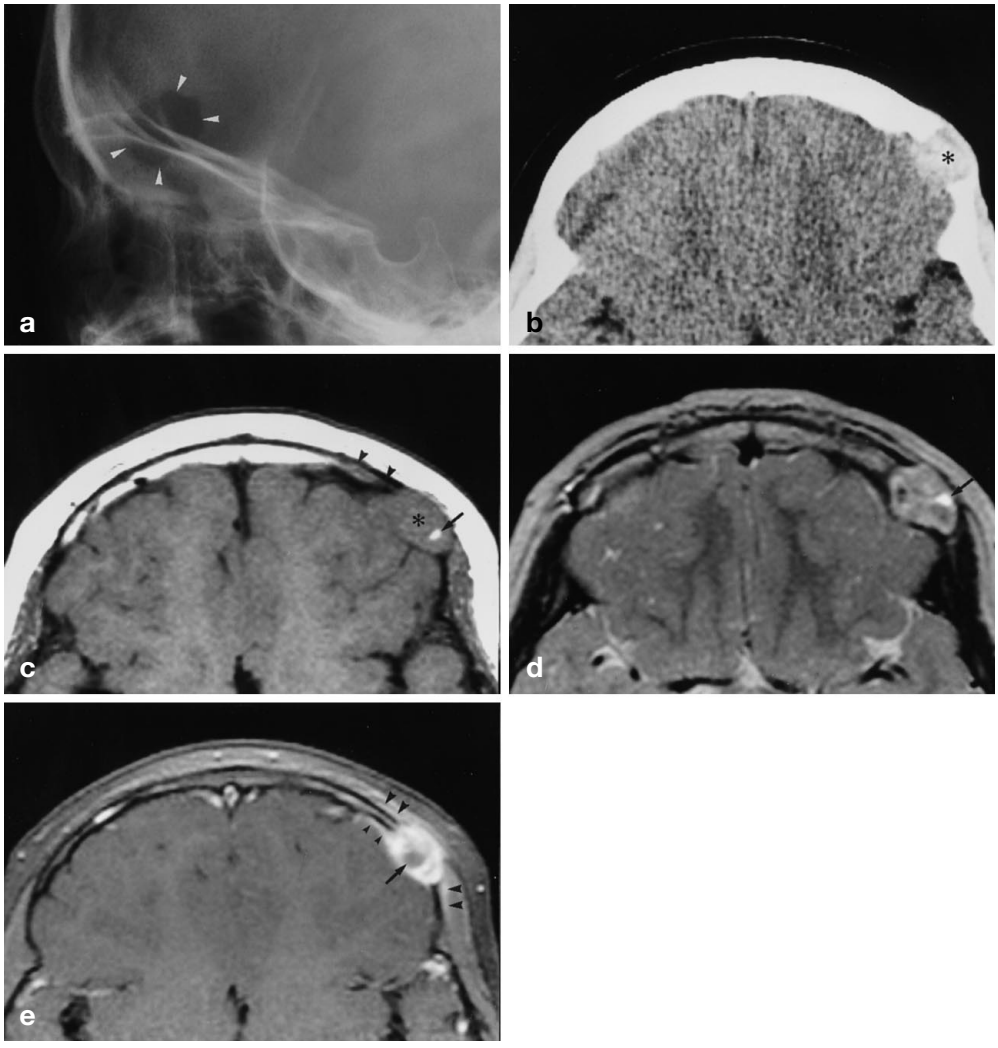

Fig. 1 a–e Case 2. **a** Skull film, lateral projection. A rounded osteolytic lesion with an irregular, nonsclerotic rim is seen in the frontal bone *(arrowheads)*. **b** CT. The frontal bone eosinophil granuloma is demonstrated as slightly denser lesion compared to grey matter of the underlying brain *(*)*. **c** T1-weighted image. The lesion is biconvex and isointense with grey matter *(*)*. A small high-signal area is seen *(arrow)*. Signal from the adjacent bone marrow is decreased *(arrowheads)*. **d** T2-weighted image. The lesion gives heterogeneously higher signal than brain, similar to that of subcutaneous fat. A small higher-signal portion, corresponding to the small high-signal area in **c,** is seen *(arrow)*. **e** Contrast-enhanced T1-weighted image with fat-suppression. The lesion enhances markedly, with a less enhancing portion *(arrow)*. A dural tail of enhancement *(small arrowheads)* and reactive galeal enhancement *(large arrowheads)* are also seen

Table 1 Clinical, radiographic and scintigraphic features

Case	Age/sex (years)	Length of history (months)	Chief complaint	Side	Craniogram					Scintigram	
					Involved bone	Size (mm)	Configuration	Sclerotic rim	Button sequestrum	Bone (Tc-MDP)	Ga-67
1	2/M	1	A lump with tenderness	Right	Parietal	23–40	Geographic	–	–	+ (circular)	–
2	6/M	1	A lump with pain	Left	Frontal	13–18	Oval	–	–	not available	not available
3	9/F	1	A lump with tenderness	Left	Frontal	20–30	Lobulated	–	–	+ (circular)	+ (nodular)
4	10/M	1	A lump with pain	Left	Parietal	20	Round	–	–	+ (circular)	–

+, positive, –, negative

Table 2 CT and MRI features [(+) positive, (++) marked, (–) negative, > hyperdense or hyperintense, G grey matter, G/W grey or white matter, * hypodense or hypointense area in lesion, ** small and markedly hyperintense area in lesion]

Case	CT					MRI										
	Density	Enhancement	Bevelled edge	Sclerotic rim	Button sequestrum	Configuration	T1WI	T2WI	Diffusion WI	Enhancement	Less enhanced portion	Dural enhancement	Galeal enhancement	Muscle swelling	Dynamic study	Flarelike phenomenon
1	> G	(++)	(+) Outer > inner	(–)	(–)	Biconvex	G	> fat	G/W	(++)	(+)	(+)	(+)	(–)	Not available	(–)
2	> G	(++)	(–) Inner = outer	(–)	(–)	Biconvex	G**	Fat**	G/W**	(++)	(+)	(+)	(+)	(–)	Available	(+)
3	> G	(++)	(+) Outer > inner	(–)	(+)	Biconvex	G/W	> fat	Not available	(++)	(+)	(+)	(+)	(–)	Available	(–)
4	> G*	(++)	(+) Inner > outer	(–)	(–)	Collar-stud	G/W*	> fat	Not available	(++)	(+)	(+)	(–)	(+)	Not available	(–)

from 13 to 40 mm in diameter. They were rounded, lobulated, or geographic in configuration (Figs. 1 a, 2 a). No sclerotic rim was seen on plain films or bone-window CT. A bevelled edge was observed in three cases on bone-window CT. The outer table was more extensively destroyed than the inner in two cases, and the inner table more destroyed in one. No button sequestrum was seen on plain films. However, small residual bone fragments were seen on bone-window CT in one case. The lesions were sharply demarcated. Three were biconvex (Fig. 1 b–e), and the other had a collar-stud appearance (Fig. 2 b–e). Although the extracranial portion of one granuloma had a low-density area (Fig. 2 b), the lesions were slightly denser than grey matter on CT (Figs. 1 b, 2 b), and enhanced markedly with contrast medium.

Except for a low-signal area in the portion which was of lower density on CT (Fig. 2 c), all lesions were isointense with grey and/or white matter on T1-weighted MRI (Figs. 1 c, 2 c). A punctate high-signal area, which seemed to represent a small haemorrhagic portion, was seen in one case (Fig. 1 c); it gave high signal on fat-suppressed images. All the granulomas gave heterogeneous high signal on both proton-density and T2-weighted images. An area giving higher signal than fat was seen in all cases (Figs. 1 d, 2 d). Dynamic MRI in two cases showed rapid increase of signal intensity in the first minute, and a gradual increase over the following 2 min. Although all lesions enhanced markedly, a small less enhancing portion was demonstrated within them (Figs. 1 e, 2 e). In one case, the signal intensity of the adjacent bone marrow was decreased on T1-weighted images (Fig. 1 c).

A tail of dural enhancement was seen in all cases, and there was reactive enhancement of the overlying galea in three cases (Fig. 1 e) and swelling of adjacent muscle in one (Fig. 2 c, d). On heavily diffusion-weighted images, the lesions were isointense with grey and/or white matter.

Bone scintigraphy demonstrated a solitary calvarial lesion showing peripheral uptake with a central defect in all three cases. On gallium scintigraphy, the lesion was hot in one case, but cold in the other two.

Discussion

About 90 % of patients with eosinophil granuloma of bone present between 5 and 15 years of age [1]; there is a slight male predominance [1, 4]. Eosinophil granuloma is uncommon, and represents less than 1 % of tumour-like lesions of bone [2]. Any bone can be involved, but there is a predilection for the flat bones, with more than half of lesions occurring in the skull, pelvis, and ribs [1, 4]. The skull is most frequently involved, the calvaria more often than the base, especially the parietal region [1–3].

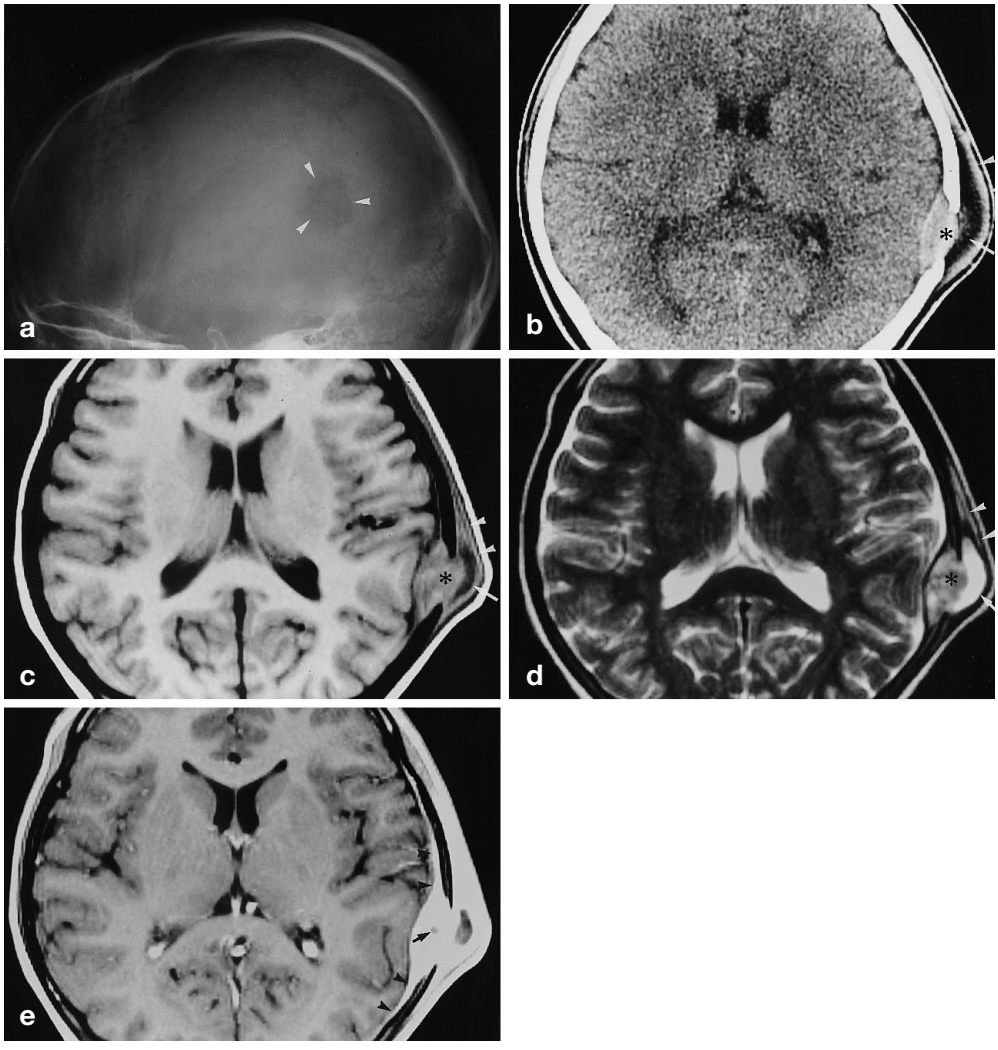

Fig. 2 a–e Case 4. **a** Skull film, lateral projection. A round osteolytic lesion of the parietal bone is demonstrated *(arrowheads)*. **b** Contrast-enhanced CT. The eosinophil granuloma in the left parietal bone is demonstrated *(*)*. Although an extracranial portion is of low density *(arrow)*, the lesion is slightly denser than the underlying brain. The inner table is more destroyed than the outer, which has a bevelled appearance. Swelling of the left temporal muscle is seen *(arrowheads)*. **c** T1-weighted image. The lesion shows a collar-stud appearance. Although the extracranial portion gives low signal *(arrow)*, the lesion is isointense with grey or white matter *(*)*. The bevelled edge is demonstrated and the overlying temporal muscle is thickened *(arrowheads)*. **d** T2-weighted image. The extracranial portion gives markedly *(arrow)*, and the lesion heterogeneously high signal *(*)*. Swelling of the overlying left temporal muscle is seen *(arrowheads)*. **e** Contrast-enhanced T1-weighted image. The lesion enhances markedly and a tail of dural enhancement is also seen *(arrowheads)*. A small less-enhancing area is seen *(arrow)*. The low-signal extracranial portion is smaller than in **c**

Radiographic appearances of osseous LCH depend on the site of involvement and the phase of the disease. In the skull, a rounded osteolytic lesion 1–4 cm in diameter is seen. Lesions may enlarge, increase in number, and coalesce to form a maplike appearance, referred to as the geographic skull. They infrequently extend across suture lines. The lesion tends to have sharp, nonsclerotic borders, with a punched-out appearance. Uneven destruction of the outer and inner cranial tables results in a bevelled edge or double contour. A "button sequestrum" or "bull's-eye" may be present within an osteolytic lesion, representing residual bone, which may be seen better on CT [1–5]. This finding was once thought to be characteristic of skeletal LCH, but may be seen in a wide variety of conditions [1, 8, 12]. Osseous perforation may result in an extradural or extracranial soft-tissue mass, demonstrated more clearly on CT [1, 5].

All our patients had a combination of these appearances. Although one had a low-density area in the extracranial portion of the lesion, the granulomas were slightly denser than grey matter on CT, an aspect which has not been emphasised in the literature. MRI is superior to other imaging methods for demonstrating bone-marrow involvement and any soft-tissue mass or inflammation [8], but there are few reports of MRI of calvarial eosinophil granuloma [6–11]. The signal intensity of eosinophil granuloma has been reported to be similar to or higher than that of muscle [8], or slightly less than that of grey matter on T1-weighted images [11], and similar to or higher than that of fat on T2-weighted images [6–11]; some cases show heterogeneity [7–9]. Marked contrast enhancement has been reported, with reactive dural enhancement [8–10]. In our cases, the lesions were isointense with grey or white matter on T1-weighted images, and gave heterogeneously high signal with a portion brighter than fat on T2-weighted images. In one case, a tiny high-signal portion was observed on all pulse sequences; this may be haemorrhage,

which is observed histologically in the early phase of eosinophil granuloma [7]. Another case showed low signal in the adjacent bone marrow on T1-weighted images. Although similar changes have been demonstrated in other sites of involvement by eosinophil granuloma in the early phases like the "flare" phenomenon of osteoblastomas, they have not been described in calvarial eosinophil granuloma [7, 8]. Although all our lesions enhanced markedly, there was a small less-enhancing portion. A nonenhancing portion in the extracranial part of one lesion was proved to be gelatinous tissue at surgery, and pathognomonic Langerhans cells were seen in this portion. Reactive dural and galeal enhancement and adjacent muscle swelling were also demonstrated. One of our cases showed a relatively large extraosseous soft-tissue mass on both sides of the skull, with collar-stud appearance [8, 9].

The differential diagnosis of a solitary lytic skull lesion in a child or young adult includes epidermoid or dermoid cysts, and other benign or malignant skull tumours, such as osteoblastoma, haemangioma, or osteogenic sarcoma [12–19]. Epidermoids and osteoblastomas usually have a sclerotic rim [12–16], haemangiomas a characteristic honycomb or sunburst pattern of bony spicules radiating from the centre of a radiolucent round or oval defect; their margins are usually not sclerotic or bevelled on plain films or CT [18]. Osteosarcomas have irregular, dense borders, or a poorly defined sclerotic area [19]. Although our observations are compatible with previously described cases of eosinophil granuloma [1–11], no single finding is specific to the disease [12–20]. However, the constellation of these findings seems to be suggestive of eosinophil granuloma. The dynamic MRI pattern might indicate its hypervascular nature.

Solitary eosinophil granulomas are more than three times as common as multiple lesions [4]. The lesions in our cases were all monostotic and solitary, and no other site of involvement was demonstrated on a skeletal survey or scintigraphy. Most bony lesions can be detected on plain radiographs. However, scintigraphy may reveal additional lesions, especially in complex bones such as the skull, mandible, and pelvis [21]. It has been suggested that a skeletal survey and radionuclide imaging should be done routinely in patients with eosinophil granuloma [21]. Although diffuse pulmonary uptake of Ga-67 citrate is documented [22], focally increased uptake has rarely been reported in osseous lesions [23]. We found a single reported case of eosinophil granuloma showing an area of markedly increased uptake of Ga-67 citrate in a lesion of the body of the sternum. Tomography demonstrated a lytic lesion with a pronounced sclerotic reaction at the periphery, and circular accumulation of Tc-99m-MDP, with a central area of markedly reduced concentration [23]. Our patient demonstrating intense accumulation of Ga-67 citrate showed no sclerotic rim on radiography or CT. In the other two cases, no uptake of Ga-67 citrate was seen. The mechanism of concentration of Ga-67 citrate in infective and neoplastic lesions is poorly understood [22]. There is a report of radiologically typical epidermoid tumours, which showed intense concentration of Tc-99m-MDP, and faint accumulation of Ga-67 citrate [24].

Intracranial epidermoid cysts give markedly high signal on diffusion-weighted images [25]. Our two cases did not do so, except in a small haemorrhagic portion. Diffusion-weighted imaging could readily differentiate eosinophil granuloma from epidermoid of the skull.

References

1. Stull MA, Kransdorf MJ, Devaney KO (1992) From the archives of the AFIP, Langerhans cell histiocytosis of bone. Radiographics 12: 801–823
2. Wells CPO (1956) The button sequestrum of eosinophilic granuloma of the skull. Radiology 67: 746–747
3. Ochsner SF (1966) Eosinophilic granuloma of bone, experience with 20 cases. AJR 97: 719–726
4. David R, Oria RA, Kumar R, Singleton EB, Lindell MM, Shirkhoda A, Madewell JE (1989) Radiologic features of eosinophilic granuloma of bone. AJR 153: 1021–1026
5. Mitnick JS, Pinto RS (1980) Computed tomography in the diagnosis of eosinophilic granuloma. J Comput Assist Tomogr 4: 791–793
6. Murayama S, Numaguchi Y, Robinson AE, Richardson DE (1988) Magnetic resonance imaging of calvarial eosinophilic granuloma. CT 12: 251–252
7. Beltran J, Aparisi F, Bonmati LM, Rosenberg ZS, Present D, Steiner GC (1993) Eosinophilic granuloma: MRI manifestations. Skeletal Radiol 22: 157–161
8. De Schepper AMA, Ramon F, Van Marck E (1993) MR imaging of eosinophilic granuloma: report of 11 cases. Skeletal Radiol 22: 163–166
9. Goldberg HI, Lavi E, Atlas SW (1996) Extra-axial brain tumors. In: Atlas SW (ed) Magnetic resonance imaging of the brain and spine, 2nd edn. Lippincott-Raven, Philadelphia, pp 423–487
10. Flores II LG, Hoshi H, Nagamachi S, Ohnishi T, Watanabe K, Fukiyama J, Nao-i N, Sawada A (1995) Thallium-201 uptake in eosinophilic granuloma of the frontal bone: comparison with technetium-99m-MDP imaging. J Nucl Med 36: 107–110
11. Caresio JF, McMillan JH, Batnitzky S (1991) Coexistent intra- and extracranial mass lesions: an unusual manifestation of histiocytosis X. AJNR 12: 82
12. Kroon HM, Schurmans J (1990) Osteoblastoma: clinical and radiologic findings in 98 new cases. Radiology 175: 783–790
13. Garcia J, Lagier R, Hoessly M (1982) Computed tomography-pathology correlation in skull epidermoid cyst. J Comput Assist Tomogr 6: 818–820

14. Demaerel Ph, Wilms G, Lammens M, Nuttin B, Plets Ch, Baert AL (1991) Extradural epidermoid tumor of the frontal bone. Neuroradiology 33: 349–351
15. Boyko OB, Scott JA, Muller J (1994) Intradiploic epidermoid cyst of the skull: case report. Neuroradiology 36: 226–227
16. Arana E, Latorre FF, Revert A, Menor F, Riesgo P, Liaño F, Diaz C (1996) Intradiploic epidermoid cysts. Neuroradiology 38: 306–311
17. Pumar J, Otero E, Castiñeira A, Alvarez M, Arrojo L, Gelabert M, Vidal J (1993) Intradiploic epidermoid tumor of the occipital bone: X-ray, CT, MR findings. Eur Radiol 3: 183–185
18. Bastug D, Ortiz O, Schochet SS (1995) Hemangiomas in the calvaria: imaging findings. AJR 164: 683–687
19. Kornreich L, Grunebaum M, Ziv N, Cohen Y (1988) Osteogenic sarcoma of the calvarium in children: CT manifestations. Neuroradiology 30: 439–441
20. Bourekas EC, Cohen ML, Kamen CS, Tarr RW, Lanzieri CF, Lewin JS (1996) Malignant hemangioendothelioma (angiosarcoma) of the skull: plain film, CT, and MR appearance. AJNR 17: 1946–1948
21. Kumar R, Balachandran S (1980) Relative roles of radionuclide scanning and radiographic imaging in eosinophilic granuloma. Clin Nucl Med 5: 538–542
22. Makhija MC, Davis G (1984) Gallium-67 imaging in pulmonary eosinophilic granuloma. Clin Nucl Med 9: 139–142
23. Taillefer R, Levasseur A, Robillard R (1981) Ga-67 imaging in eosinophilic granuloma. Clin Nucl Med 6: 270–271
24. Makhija MC, Vincent NR (1980) Scintigraphy in epidermoid tumor of the skull. Clin Nucl Med 5: 122–124
25. Tsuruda JS, Chew WM, Moseley ME, Norman D (1990) Diffusion-weighted MR imaging of the brain: value of differentiating between extraaxial cysts and epidermoid tumors. AJNR 11: 925–931